C. R. Geoscience 350 (2018) 119–129

Contents lists available at ScienceDirect

Comptes Rendus Geoscience

www.sciencedirect.com

Hydrology, Environment (Surface Geochemistry)

Mineralogical and geochemical features of alluvial sediments from the Lobo watershed (Southern Cameroon): Implications for rutile exploration

Jules Mbanga Nyobe [a], Elisé Sababa [a,*], Elie Constantin Bayiga [b], Paul-Désiré Ndjigui [a]

[a] Department of Earth Sciences, University of Yaoundé-1, P.O. Box 812, Yaoundé, Cameroon
[b] Department of Earth Sciences, University of Douala, P.O. Box 24157, Douala, Cameroon

ARTICLE INFO

Article history:
Received 27 June 2017
Accepted after revision 29 August 2017
Available online 1 February 2018

Handled by François Chabaux

Keywords:
Alluvial sediment
Geochemistry
Rutile-exploration
Lobo watershed
Yaoundé Group

ABSTRACT

This paper is focused on the morphological, mineralogical, and geochemical features of alluvial sediments from the Neoproterozoic Pan-African belt to explore rutile. The fine-grained sediments, which contain a large proportion of rutile, are made up of quartz, rutile, zircon, brookite, tourmaline, andalusite, and kyanite. The high SiO_2 and TiO_2 contents highlight the predominance of silica minerals in the alluvia from the humid tropical zone. La/Sc, La/Co, Th/Sc and Zr/Cr ratios reflect the contribution of felsic and mafic sources. The highest Ti contents, which occur at the outlet of the Lobo watershed, indicate the resistance of rutile. The REE distribution could be linked to the heavy mineral sorting. The low $(La/Yb)_N$ ratios and high Zr contents are attributed to the high proportion of zircon. Chondrite-normalized REE patterns indicate high felsic sources, which are the regional rocks. Ultimately, the Yaoundé Group constitutes a favorable potential target for further rutile exploration.

1. Introduction

Rutile occurs in metamorphic, igneous rocks, mantle xenoliths, lunar rocks, meteorites, and crystallizes, in a wide range of temperature and pressure, mostly in high-grade metamorphic rocks (Miller et al., 2007; Zack et al., 2002), some granulites and gneisses (Stendal et al., 2006). Rutile is commonly exploited in clastic sediments as a stable heavy mineral that constitutes an important source of Ti (Meinhold, 2010; Tonje et al., 2014). The high mechanical and chemical stability of rutile during weathering, transportation, and diagenesis (Morton and Hallsworth, 1999) makes rutile an important tool for source-rock characterization in provenance studies (Zack et al., 2004). The composition of the sediments depends mostly on that of their source rocks and on the intensity of chemical weathering (Ahmad et al., 2014; Silva et al., 2016). Some parameters such as transport, deposition, and diagenesis can also modify the sediments during the sedimentation cycle (Morton and Hallsworth, 1999).

Alluvial sediments are commonly composed of quartz, feldspars and mica as major constituents, and of minor amounts of heavy minerals such as zircon, rutile, tourmaline, garnet, epidote, and chrome spinel (Meinhold et al., 2008). Alluvium can contain valuable ores such as gold (Moufti, 2014; Muhammad and Mansoor, 2015), platinum (Cook and Fletcher, 1993; Duran et al., 2015; Traoré et al., 2006), and a wide variety of gemstones (Le Goff et al., 2010; Simonet et al., 2008). Major, trace, and rare earth element

* Corresponding author.
E-mail addresses: sababae@yahoo.fr, esababa@uy1.uninet.cm (E. Sababa).

http://dx.doi.org/10.1016/j.crte.2017.08.003
1631-0713/

geochemistry and their elemental ratios are useful to provide information about the sediments' origin as well as the weathering conditions of the source areas. The major element geochemistry of sediments tends to reflect the source rock composition (Armstrong-Altrin et al., 2012) and weathering intensity (Shao and Yang, 2012; Šmuc et al., 2015). Trace elements such as REE, Y, Th, Zr, Hf, Nb and Sc are suited to investigate the sediments' provenance (Martins et al., 2012; Prego et al., 2012), because of their relatively low mobility during the sedimentary processes (Ahmad et al., 2014; Asadi et al., 2013). Due to their coherent geochemical behavior and low solubility, the rare earth elements (REE) are considered good tracers to identify the sources of terrestrial materials (Song and Choi, 2009). The source rock composition is the primary control on REE composition, with weathering processes playing only a minor role (Armstrong-Altrin et al., 2012).

The occurrence of rutile in the Yaoundé Group from the Neoproterozoic Pan-African Belt is known in alluvial and residual deposits since the last century (Maurizot et al., 1986; Owona et al., 2011). Its origin is still uncertain in the whole area (Stendal et al., 2006; Zack et al., 2002), and according to Silva et al. (2016), there is generally enrichment by trace elements in the fine-grained sediments. Thus, given the important role that rutile plays in both economic and fundamental geology, we report in this paper the morphological, mineralogical, and geochemical features of the fine-grained sediments (0.5 to 0.8 mm) from the Lobo watershed to estimate its metallogenic importance and discuss the provenance of rutile-bearing sediments.

2. Geographical and geological setting

The Lobo watershed is situated northeast of Yaoundé (Fig. 1). It is characterized by a humid tropical climate with four seasons. The study site corresponds to a transitional zone between rainforest and savanna (Letouzey, 1985). The area belongs to the Yaoundé Group and its morphology is dominated by smooth-rocky hills with large convex slopes and swampy valleys. The Yaoundé Group is an allochthonous unit emplaced onto the Congo craton, which constitutes a part of the Central African Mobile Zone (CAMZ) and is Late Neoproterozoic based on its Th–U–Pb age determined on monazite (613 ± 33 Ma) (Owona et al., 2011; Penaye et al., 1993; Toteu et al., 2001). The micaschists, quartzites and gneisses are intensively folded. These characteristics favor weathering, which leads to thick ferrallitic soils and swampy hydromorphic soils around the valleys. The whole swamp is overlain by a grey clayey sandy material and essentially composed of kaolinite, smectite and residual quartz, feldspars, rutile, and zircon (Braun et al., 2005).

The assumed "rutile zone" covers the entire South Cameroon plateau. It is a gently undulating surface with altitude varying between 600 and 800 m dominated by a succession of convex or tabular hills. This vast plateau is prolonged to the south towards Gabon and to the east towards the Central African Republic (Champetier de Ribes and Aubague, 1956; Stendal et al., 2006). Two great geological formations underlie South Cameroon; the formations within the mobile zone in the North and those of the Ntem complex in the South (Champetier de Ribes and Aubague, 1956; Stendal et al., 2006). The basement is constituted of metamorphic rocks (gneisses, quartzites and schists). The Yaoundé Group is made up of two series: the Mbalmayo–Bengbis–Ayos and the Yaoundé series (Maurizot et al., 1986). Paragneisses and orthogneisses are predominant in the Yaoundé series. Rutile occurrences are known in low- and medium-grade schists, where crystals are up to a centimeter in size. In the high-grade gneisses, it is less represented and appears as fine-grained inclusions within garnet or as euhedral xenocrysts (Maurizot et al., 1986; Nzenti et al., 1988).

3. Sampling and analytical techniques

The sampling and analytical techniques including Figs. SM1 and SM2 and Tables SM1 to SM5 are presented in the supplementary data.

4. Results

4.1. Petrography and major element distribution of rocks

4.1.1. Petrography

Gneisses and micaschists are metamorphic rocks encountered within the Lobo watershed.

Gneisses outcrop as blocks and as paved surfaces. The rock is interstratified, dark grey, with variable grain sizes. Under the microscope, the rock shows compositional banding and heterogranular granoblastic microstructures. The light bands are quartzo-feldspathic, while the dark bands are comprised of biotite, garnet, and opaque minerals. Quartz, which constitutes 25–40% of the rock, shows xenomorphic crystals preferentially oriented as polycrystalline ribbons and granule inclusions in garnet porphyroblasts. Plagioclase (10–35%) shows massive crystals with different sizes that vary between 0.22×0.10 mm and 0.66×0.42 mm. Biotite crystals ($< 10\%$) are preferentially oriented flakes or lensoids. Biotite flakes have variable dimensions of 0.48×0.24 and 1.36×0.32 mm with other crystals found as inclusions in garnet. Garnet ($< 10\%$) shows either dispersed globular forms within the rock or as porphyroblasts containing quartz, biotite, and opaque mineral inclusions. Garnet crystals have variable diameters between 0.40 and 1.6 mm and often show corroded rims of biotite and quartz. Some garnet porphyroblasts show quartz and biotite rims. Opaque minerals (about 5%) occur as subautomorphic crystals or as inclusions in garnet.

Micaschists outcrop as paved surfaces, blocks, or domes. Micaschists, compared to gneisses, are massive, fine to medium-grained and dark grey in color. Under the microscope, the rocks are characterized by heterogranular granoblastic microstructures. Quartz crystals represent about 45%, occurring as xenomorphs and define light polycrystalline banding. Plagioclase (10–45%) is abundant, and shows plates 0.36 mm in length and 0.24 mm in width. The crystals are massive and associated with those of quartz. Garnet ($< 10\%$) is dispersed in the rock as

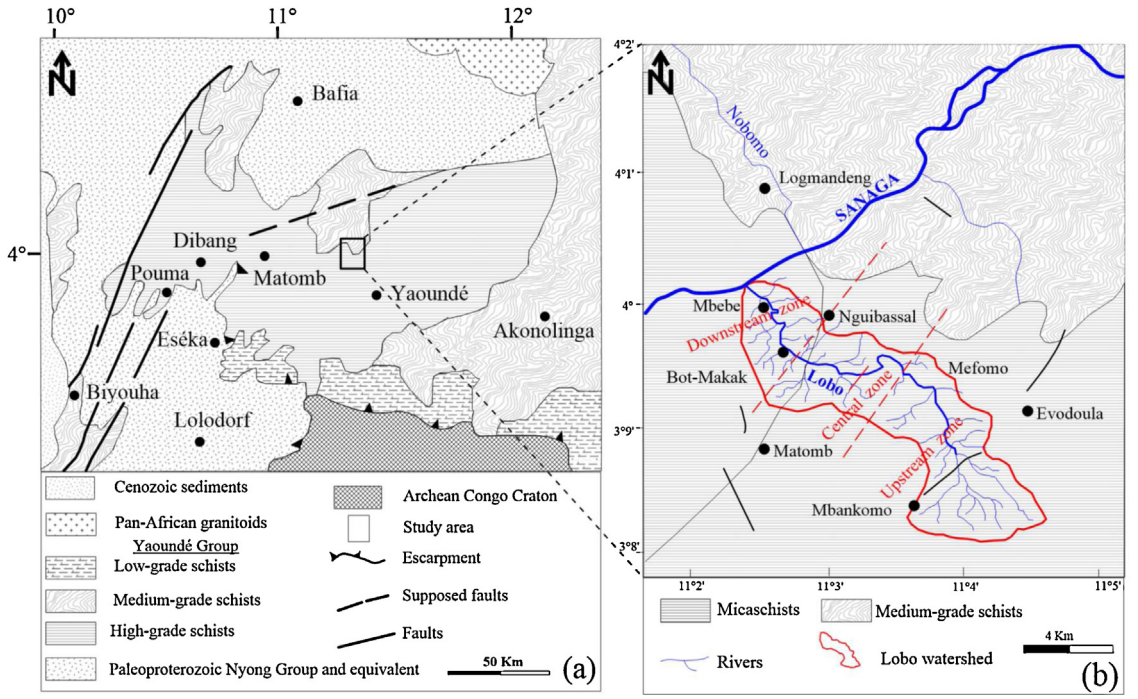

Fig. 1. a: Regional geological map of southern Cameroon (Stendal et al., 2006); b: location and geological map of Lobo watershed (Champetier de Ribes and Aubague, 1956).

porphyroblasts containing quartz, biotite, and opaque minerals as inclusions.

4.1.2. Distribution of major elements

SiO_2 contents in the rocks from the Lobo watershed vary between 62 and 69 wt.% with the lowest content in the mica-schist sample (Table SM1). Al_2O_3 contents range between 13 and 17 wt.% and those of Fe_2O_3 range between 3 and 8 wt.% (Table SM1). The MgO, CaO, Na_2O, K_2O, MnO and P_2O_5 contents are low. Micaschists are characterized by the highest content in TiO_2 (1.53 wt.%). The loss on ignition values are significant, ranging between 1 and 4 wt.% (Table SM1). Correlations of TiO_2 with SiO_2 and K_2O are negative (Fig. 2a and b). However, TiO_2 has positive correlation with MgO, Fe_2O_3, P_2O_5 and MnO (Fig. 2c–f), and no significant correlation with Al_2O_3 and CaO (Fig. 2g and h).

4.2. Mineralogy and geochemistry of alluvial sediments

4.2.1. Mineralogical characterization

Sample separation and heavy mineral extraction show that the fine fraction (0.5 to 0.8 mm) contains a large proportion of rutile. Macroscopic observations of the concentrates, i.e. the fine-grained sediments, reveal that they are mostly composed of quartz, rutile and, to a lesser extent, of opaque minerals (Fig. SM2a and b). Rutile as well as quartz contours are often very irregular.

The heavy mineral assemblage is made up of rutile, zircon, brookite, tourmaline, andalusite, and kyanite (Fig. SM2c and d). They appear mostly in the downstream zone, where kyanite is absent. They are tabular, rounded, or slightly elongated. The tabular grains are angular, whereas elongated and rounded grains are sub-blunt to prismatic.

The mineral assemblage of the fine fractions obtained by XRD analysis is made up of quartz, rutile, zircon, muscovite, and ilmenite (Table SM2).

4.2.2. Geochemical characterization of alluvial sediments

4.2.2.1. Distribution of major elements. TiO_2 and SiO_2 are the major elements with the highest contents in the Lobo watershed sediments. TiO_2 contents vary from 9 to 57 wt.% and those of SiO_2 are between 21 and 81 wt.% (Table SM3). The SiO_2 contents decrease from the upstream to the downstream zone, while TiO_2 contents have an opposite trend. The concentrations in Al_2O_3 (1–21 wt.%) and Fe_2O_3 (3–20 wt.%) are variable (Table SM3). Several samples have CaO contents higher than 1 wt.%. Other oxides (MnO, MgO, Na_2O, K_2O, and P_2O_3) have low contents (Table SM3). TiO_2 shows high negative correlations with SiO_2, and K_2O (Fig. 3a and b). The negative correlations with Al_2O_3 are observed in the upstream zone (Fig. 3c). Conversely, TiO_2 possesses no significant correlations with Fe_2O_3 and very slight positive ones with MnO (Fig. 3d and e). The behavior of MgO compared to TiO_2 depends on the zone; both oxides have positive correlations in the upstream zone and negative correlations in the central zone (Fig. 3f).

The highest TiO_2 concentrations are in the downstream zones of the Lobo watershed, except for the DjA sample, with a TiO_2 content of 18.2 wt.%. The distribution map of the Ti concentrations of the fine-grained sediments in the

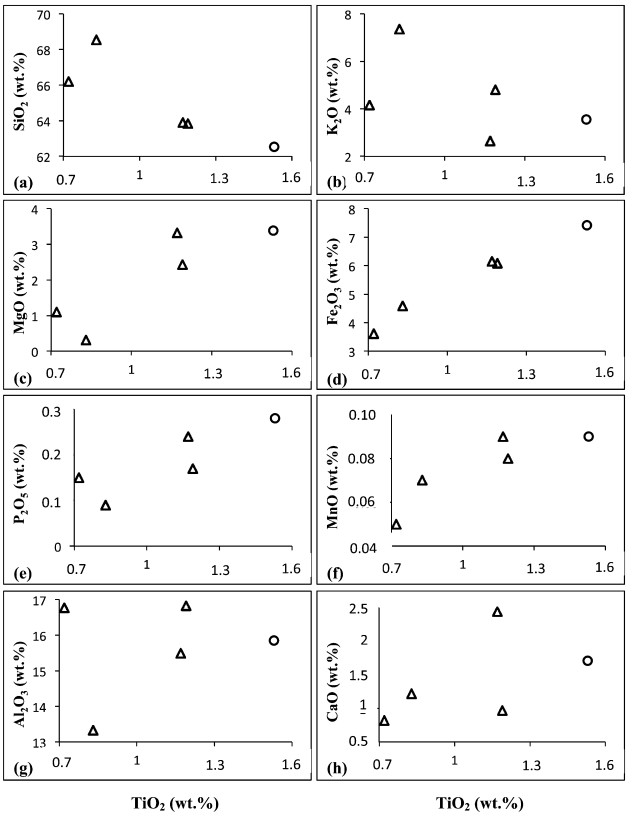

Fig. 2. Binary diagrams of TiO_2 versus some major elements for the Lobo rocks: a: TiO_2 vs. SiO_2; b: TiO_2 vs. Al_2O_3; c: TiO_2 vs. K_2O; d: TiO_2 vs. Fe_2O_3; e: TiO_2 vs. MgO; f: TiO_2 vs. MnO; g: TiO_2 vs. P_2O_5; h: TiO_2 vs. CaO.

Lobo watershed shows that the TiO_2 contents increase from the upstream to the downstream zones (Fig. 4).

The Chemical Index of Alteration (CIA) is an indicator of the degree of the weathering (McLennan, 1993; Nesbitt and Young, 1984). It is defined as $CIA = Al_2O_3/(Al_2O_3 + CaO^* + Na_2O + K_2O) \times 100$ (molar contents, with CaO^* being the CaO content in the silicate fraction of the sample). If the CaO molar content is greater than that of Na_2O, CaO^* is assumed to be equivalent to Na_2O, whereas if the CaO molar content is less than that of Na_2O, the measured CaO content can be used for CaO^* (Shao et al., 2012; Šmuc et al., 2015). An unweathered rock has the lowest CIA (about 50% or less). During weathering, cations are lost from the material and CIA increases to reach 100. CIA values vary between 75 and 98% in the fine-grained sediments from the Lobo watershed, and they increase from the upstream zone of the basin towards the central and the downstream zones (Table SM3).

4.2.2.2. Distribution of trace elements. Amongst the trace elements suite, Zr has the highest contents (from 662 to more than 1450 ppm) (Table SM4). The Cr contents vary between 117 and 1056 ppm; concentrations in V (more than 370 ppm) and Nb (more than 277 ppm) are very high compared to those of the other trace elements (Table SM4). Many trace elements like Cu (up to 59 ppm), Ba (8–88 ppm), Y (7–110 ppm), Pb (4–27 ppm), Th (5 to more than 109 ppm), Ta (11–103 ppm) and W (7–71 ppm) have significant and variable concentrations (Table SM4). In addition, Sn (higher than 14 ppm) and Hf (from 15 to more than 29 ppm) possess high values. The contents in Ni (4–16 ppm), Co (3–17 ppm), Sc (5–63 ppm), Sr (5–23 ppm), and Ga (2–21 ppm) are moderate. The concentrations in Zn and Li come up to 1286 and 71 ppm, respectively, in the downstream zone. The uranium content reaches 66 ppm in the upstream zone. Other trace elements (Li, Rb, Mo, U, Ta, Be, Cd, Cs, Sb and Sn) have low concentrations, but higher than the detection limits (Table SM4). Otherwise, TiO_2 is positively correlated with Cr, Ta, W and Sc (Fig. 5a–d), and negatively with Ba and Y (Fig. 5e and f).

La/Co and Zr/Cr ratios are high in the whole watershed (Table SM4). La/Sc and Th/Sc ratios have a contrasting behavior. Their values are high in the upstream zone, while, in the central and downstream zones, there are some samples with La/Sc and Th/Sc ratios lower than 1 (Table SM4). This reveals the Sc high contents in the central and downstream zones.

4.2.2.3. Distribution of rare-earth elements. The total REE content varies between 28 and 1752 ppm (Table SM5). Globally, the highest values are obtained in the upstream zone. The highly concentrated REE include La, Ce, Pr, Nd,

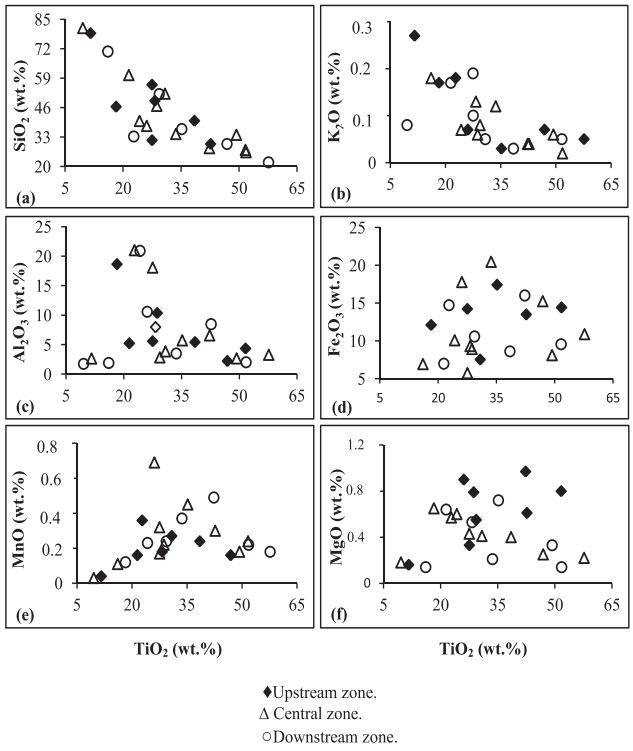

Fig. 3. Binary diagrams of TiO_2 versus some major elements for the Lobo fine-grained sediments: a: TiO_2 vs. SiO_2; b: TiO_2 vs. Al_2O_3; c: TiO_2 vs. Fe_2O_3; d: TiO_2 vs. MgO; e: TiO_2 vs. MnO; f: TiO_2 vs. K_2O.

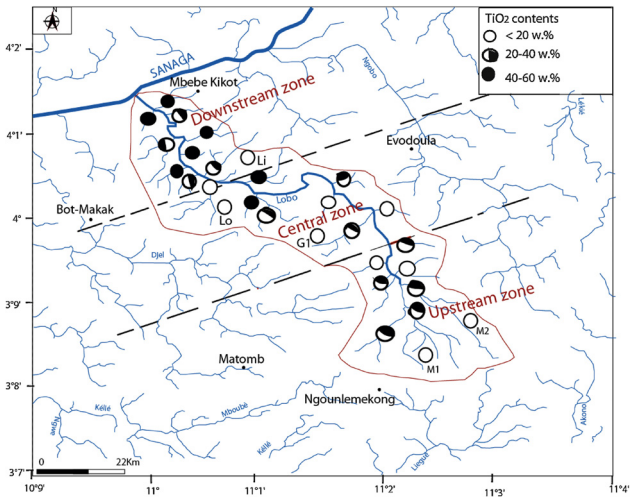

Fig. 4. Distribution map of the Ti-concentrations in the Lobo fine-grained sediments (M1, M2, LO, G1 and Li are rock samples).

and Sm (Table SM5). The LREE/HREE ratio values are both high and variable (1.85–30.30; Table SM5). The highest values are obtained in the upstream zone, while the lowest are in the central part of the Lobo watershed. Most of the samples exhibit negative Eu anomalies (Table SM5). The upstream zone shows the highest $(La/Yb)_N$ ratios and the lowest $TiO_2/((La/Yb)_N)$ and TiO_2/(LREE/HREE) ratios (Table SM5).

PAAS-normalized (McLennan, 1989) REE patterns exhibit: (i) LREE enrichment with negative Eu anomalies for upstream zone (Fig. 6a); (ii) and the central and downstream zones show contrasting REE behavior; some samples are characterized by LREE enrichment and negative Eu anomalies, while others are enriched in HREE with no Eu anomalies (Fig. 6c and e). Conversely, the chondrite-normalized (McDonough and Sun, 1995) REE

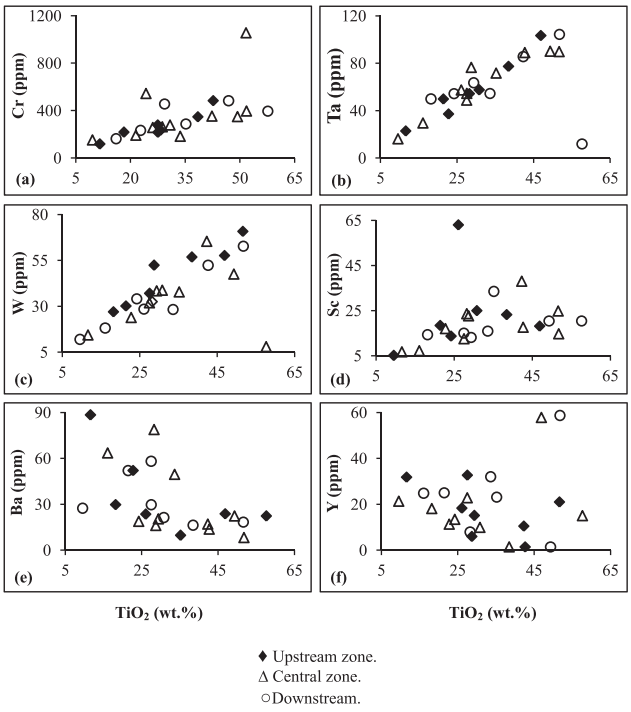

Fig. 5. Binary diagrams of TiO_2 versus trace elements for the Lobo fine-grained sediments: a: TiO_2 vs. Cr; b: TiO_2 vs. Ta; c: TiO_2 vs. W; d: TiO_2 vs. Sc; e: TiO_2 vs. Ba; f: TiO_2 vs. Y.

patterns portray a similar trend in each zone. According to chondrite-normalization, LREE enrichment and negative Eu anomalies decrease from the upstream to the downstream zones (Fig. 6b, d and f).

The LREE behavior in the Lobo watershed reveals a similar trend according to the PAAS-normalized spectra (McLennan, 1989) (Fig. 7a) as well as the chondrite-normalized spectra (McDonough and Sun, 1995) (Fig. 7b). The HREE patterns show a contrasting behavior for both normalizations (Fig. 7a and b). These normalizations confirm the high LREE/HREE and $(La/Yb)_N$ ratios in the upstream zone compared to the central and downstream ones.

5. Discussion

5.1. Petrography and geochemistry of rocks

Gneisses and micaschists from the Lobo area have almost the same mineralogical composition mainly made up by quartz, feldspars, biotite, garnet, and opaque minerals. The differences in the mineralogical and textural features could be linked to varying degrees of metamorphism (Maurizot et al., 1986). These rocks have high SiO_2 and low MgO contents, and they could result from the metamorphism of a felsic protolith (Bouyo et al., 2015). The relative high Fe_2O_3 contents and loss on ignition could be due to the slightly weathered state of the rocks (Schwertmann, 1971). The significant TiO_2 contents must be attributed to the presence of rutile, which occurs as fine-grained inclusions in the rocks of the Yaoundé Group (Maurizot et al., 1986; Nzenti et al., 1988). The positive correlations between TiO_2 and Fe_2O_3, MgO, MnO, and P_2O_5 (Fig. 2c–f) reveal that Ti, Fe, Mg, Mn and P might accumulate in the same minerals. The negative correlations between TiO_2 and SiO_2 (Fig. 2a) are probably due to the high SiO_2 concentrations. In fact, the TiO_2 content is supported by rutile and brookite, and the high SiO_2 is linked to the proportion of quartz.

5.2. Mineralogy and geochemistry of alluvial sediments

5.2.1. Mineralogical characterization

The mineral assemblage is dominated by quartz, rutile, and zircon. This mineral assemblage is characteristic of hydromechanical transport. The high proportion of rutile in the alluvia is relative to the stability of rutile during the weathering process as well as in the alluvial environment (Morton and Hallsworth, 1999). Contrary to Tonje et al. (2014), it is the fine-sized sand, which was called sterile that contains an important amount of rutile. The fine grains may represent broken fragments from fracturing of larger grains during a long transportation, or a primary conserved feature. Some of the fine grains have retained their original shape (short prisms), and it implies that they were not deposited very far from their source area.

The grain size of hard, weathering resistant displaced and deposited minerals such as rutile, quartz, tourmaline, and zircon highly depends on the textural features of their source rocks (Bassis et al., 2016; Roux and Rojax, 2007). The heavy minerals, including rutile, are angular and, to a lesser extent, sub blunt to prismatic in features. The angular nature is a conserved primary relic features during transportation. These angular grains may

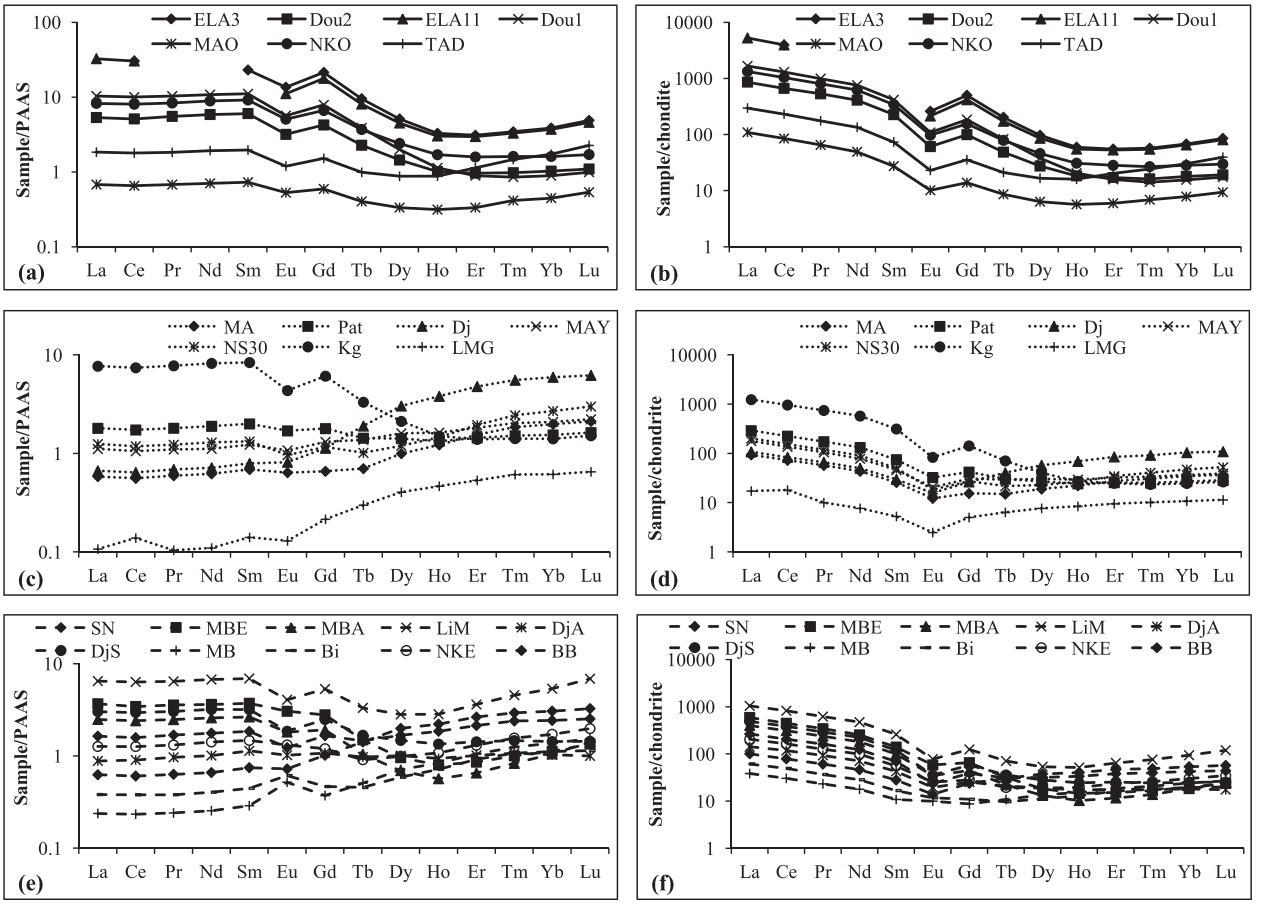

Fig. 6. PAAS- and chondrite-normalized REE patterns for Lobo fine-grained sediments: a and b: upstream zone; c and d: central zone; e and f: downstream zone. The LREE contents in some samples higher than the maximum value that the techniques determine are not reported: La (> 1380 ppm), Pr (> 240 ppm), Nd (> 760 ppm) and Sm (> 128 ppm). These values are obtained in the upstream zone of the Lobo watershed.

probably be a product of local sedimentation. The blunt nature of some rutile grains may be due to long hydromechanical transportation (Kanouo et al., 2012). The provenance of the rutile in the Lobo watershed seems contrasted.

5.2.2. Geochemical characterization

The Chemical Index of Alteration (CIA) is frequently used as parameters of the weathering characteristics and source composition of sedimentary rocks (Bhat and Ghosh, 2001; Fedo et al., 1995; Long et al., 2012). The CIA values (75–98%) from the sediments of the Lobo watershed indicate that the source rocks were strongly weathered in ferrallitic soils, which were intensively eroded (Liu et al., 2016). The high CIA values could also be linked to the abundant compositionally mature alumina-rich minerals in the source (Fedo et al., 1995; Nesbitt and Young, 1982). There is a spatial variation in the CIA values, with the lowest values in the samples from the upstream zone and the highest CIA values in the samples from the downstream zone. These differences between the CIA values may be due to the effect of sediments weathering during river transport. The variation in the CIA values in the same river due to hydrodynamic sorting was also reported by Shao and Yang (2012).

The alluvial sediments from the Lobo watershed exhibit high SiO_2 and TiO_2 contents. This is highlighted by the predominance of silica-minerals such as quartz, zircon, tourmaline and andalusite in the source rock. In fact, the high SiO_2 and TiO_2 contents characterize the intensity of pre- and post-depositional chemical weathering (Nesbitt and Young, 1984). The high TiO_2 contents in the fine-grained sediments attest to the predominance of residual bearing Ti-minerals such as rutile and brookite. Otherwise, the highest TiO_2 contents observed at the downstream zone highlight the abundance of rutile as a resistant mineral during sedimentary processes. The erosion processes and the morphology of the watershed favor Ti-accumulation in the downstream zone. The low Ti content in sample DjA from the downstream zone of the watershed is linked to the low rutile mineral amount and that could be due to local features. The low K_2O contents are due to the lack of micas, which are concentrators of K_2O (Silva et al., 2016). The SiO_2 and Fe_2O_3 contents compared to those of TiO_2 show an opposite trend in the whole watershed. This is due to the CIA values that increase from

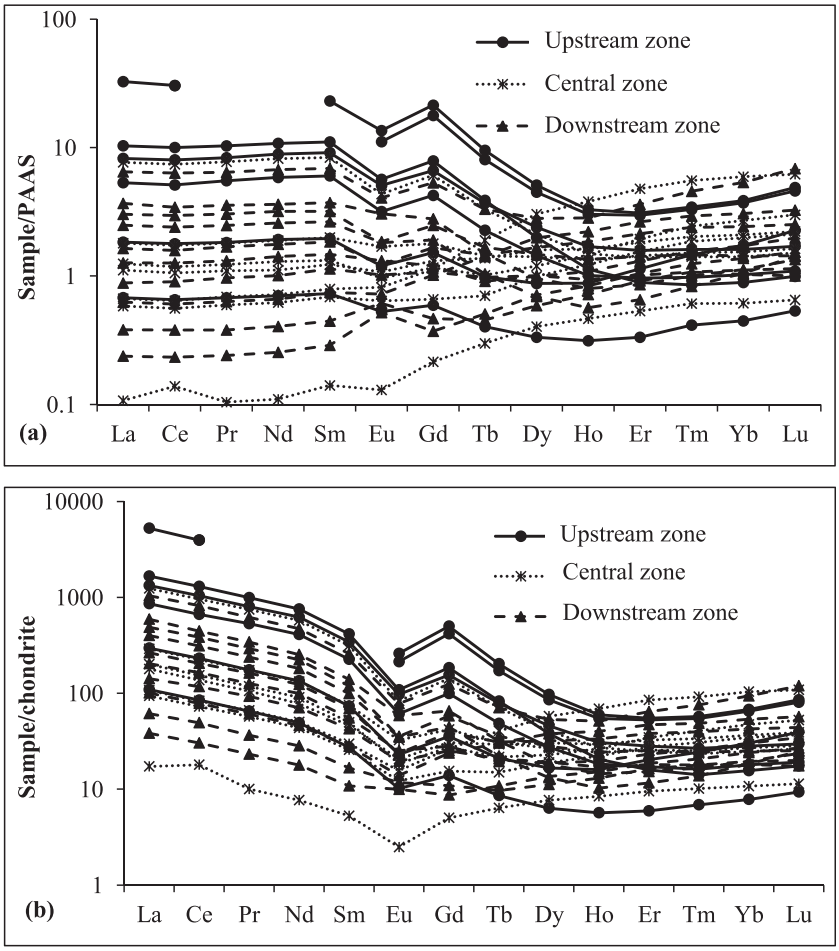

Fig. 7. REE patterns for the Lobo fine-grained sediments: a: PAAS-normalization (McLennan, 1989); b: Chondrite-normalization (McDonough and Sun, 1995). As in Fig. 6, the LREE contents in some samples higher than the maximum value that the techniques determine are not reported: La (> 1380 ppm), Pr (> 240 ppm), Nd (> 760 ppm), and Sm (> 128 ppm).

the upstream to the downstream zone as well as the source rocks and confirms the resistance of rutile in an agitated aqueous milieu. The variable Al contents may be linked to the distribution of andalusite. The complex correlations between TiO_2 and other major elements can be linked to the CIA variation and sorting process. However, the slight positive correlations between TiO_2 and Fe_2O_3, MgO, and MnO (Fig. 3) suggest that rutile might contain little amounts of Fe, Mg, and Mn due to the presence of minerals as inclusions (Kanouo et al., 2012; Meinhold, 2010). The relative abundance of trace elements such as Cr, V, Zr and Nb might be attributed to mineral sorting (Kasanzu et al., 2008). The high contents in Fe_2O_3, TiO_2, V, and Cr could also be due to the presence of ilmenite (Silva et al., 2016). The low contents of most trace elements reflect the high content of quartz, which causes a dilution effect. The lack of minerals such as micas and feldspars is responsible for the low contents in several elements like Rb, Ba, and Sr. These trace elements (e.g., Rb and Ba) substitute K in the micas. K-feldspar concentrates Rb, Ba and plagioclase concentrates Sr (White, 2013). The high Zr contents might be related to the high zircon proportion in the heavy mineral concentrates. Rutile is the most abundant mineral in the samples apart from quartz, and Ti is positively correlated with some trace elements (Cr, Ta, W and Sc; Fig. 5a, d and f). This confirms the facts that, rutile can possess a wide range of trace elements (Meyer et al., 2011; Zack et al., 2002). In fact, the formula of rutile is TiO_2, with possible substitutions for Ti^{4+} by Nb^{5+}, Ta^{5+}, Zr^{4+}, Hf^{4+}, Cr^{3+}, and Fe^{3+} (Cherniak et al., 2007; Tanis et al., 2016). Otherwise, Cr-rich rutile is a powerful tool for diamond exploration (Malkovets et al., 2016).

The high REE contents may be explained by the presence of REE-enriched heavy minerals (Wang et al., 2014). Chondrite-normalized (McDonough and Sun, 1995) REE patterns exhibit pronounced negative Eu anomalies and relatively flat heavy rare earth patterns, which is similar to those of upper crust (Silva et al., 2016). Most of the upstream sediments have similar and uniform REE patterns with LREE-abundance relative to chondrite (McDonough and Sun, 1995) and PAAS (McLennan, 1989). Similarities in the REE contents, REE fractionation, and europium anomalies indicate that the source of REE in the sediments is the same and that their source is the

regional rocks (Silva et al., 2014). Compared to the PAAS, the sediments from the central and downstream zones exhibit a contrasting behavior. Some samples show LREE enrichment and negative Eu anomalies, while others possess HREE-enrichment values with no Eu anomalies (Fig. 6a, c and e). The LREE- or HREE-enrichment could be attributed to the zircon distribution. High LREE/HREE and low $(La/Yb)_N$ ratios is linked to the proportion of zircon and the nature of REE mineral-bearers. In fact, zircon incorporates HREE preferentially over LREE, leading to HREE abundance and low $(La/Yb)_N$ (Li et al., 2005). The $(La/Yb)_N$ ratios show that REE are more fractionated in the upstream zone. The observed LREE/HREE and $(La/Yb)_N$ ratios variations may suggest an effect of heavy minerals sorting with a significant enrichment of dense and resistant minerals in central and downstream zones of the basin, as shown in Table SM2. This has been also highlighted by the TiO_2 contents compared to the LREE/HREE and $(La/Yb)_N$ ratios in the different zones of the basin (Table SM5). Many authors also reported an HREE preferential enrichment in the Fe oxyhydroxides (e.g., Borrego et al., 2005; Merten et al., 2005).

The negative Eu anomalies (Fig. 7) result generally from the weathering of feldspars (Saleh, 2007) and the reduction conditions ($Eu^{3+} \rightarrow Eu^{2+}$) (Neal and Taylor, 1989). The negative Eu anomalies could result also from the depletion of europium mineral bearers, especially accessory minerals such as monazite and apatite (Saleh, 2007). In addition, the sample preparation, which eliminates the very fine-grained part (feldspars, clays. . .) from sediment samples by washing, might contribute to the depletion of europium mineral-bearers.

5.3. Sediment provenance

According to the heavy minerals (rutile, zircon, brookite, tourmaline, andalusite and kyanite) morphology, the sediments may have two origins: (i) the grains which retained their original shape militate for a local sedimentation; and (ii) the blunt grains support the fact that the sediments are deposited very far from their source area.

The trace element geochemistry of sediments has been used by several authors to infer their provenance (e.g., Armstrong-Altrin et al., 2004, 2015; Zaid and Gahtani, 2015). Elevated values of Cr (> 150 ppm) and Ni (> 100 ppm) are suggestive of ultramafic sources (Garver et al., 1996). In this study, the sediments have high Cr and low Ni contents, indicating that likely sediments do not have an ultramafic origin. The REE patterns and the Eu anomaly values can help to understand the source of the terrigenous sediments (Ali et al., 2014; Etemad-Saeed et al., 2011; Nagarajan et al., 2011). Mafic igneous rocks contain little or lack of negative Eu anomalies, whereas felsic igneous rocks generally show negative Eu anomalies (Cullers et al., 1987). The high LREE/HREE ratios and negative Eu anomalies in the Lobo sediments indicate high felsic upper crustal sources (Bassis et al., 2016; Silva et al., 2016). As a result, the sediments in the Lobo watershed come mostly from felsic regional rocks. The differences between the CIA values in the same river may also be due to the different sources of sediments (Silva et al., 2016). Elemental ratios like La/Sc, La/Co, Th/Sc, and Zr/Cr are useful as good discriminators between mafic and felsic source rocks; La, Th and Zr are concentrated more in felsic igneous rocks, while Co, Sc and Cr have higher concentrations in mafic rocks (Ronov et al., 1974; Wronkiewicz and Condie, 1990). The high Sc contents in the central and downstream zones militate for a contribution of mafic source at least in these zones.

Rutile originated from mafic rocks is rich in Cr and poor in Nb (Zack et al., 2004). However, the fine-grained sediments, which are mostly composed of rutile in the Lobo watershed, have high Cr and Nb contents. This suggests the contribution of many different rocks such as gneisses, micaschists, quartzites, and pegmatites found in the Yaoundé Group.

6. Conclusions

Based on the morphological and geochemical features of the fine-grained alluvial sediments of the Lobo watershed in the Yaoundé Group, the following conclusions are supported:

- the Lobo fine-grained sediments are hydromechanically transported and derived from felsic source with a contribution of mafic source towards the downstream zones;
- there are two types of rutile in the Yaoundé Group: fine- and coarse-sized rutile. The fine-grains of rutile and other heavy minerals present primary conserved features that support a local sedimentation interpretation;
- the high SiO_2 and TiO_2 contents recall the predominance of silica-minerals in the alluvia from the humid tropical zone and the high resistance of rutile during supergene processes (weathering, erosion and transportation). The geochemical data of fine-grained sediments reflect their mineralogy and the regional rocks;
- the LREE/HREE and $(La/Yb)_N$ ratios are particularly high in the upstream zone. The REE behavior can be attributed to the heavy mineral sorting. The chondrite-normalized REE patterns are characterized by pronounced negative Eu anomalies and flat HREE patterns as noticed in the upper crust;
- the distribution of major and trace elements corroborates the variation of CIA values. Moreover, these data suggest that the potential of the fine-grained sediments from the Lobo watershed as rutile deposits is interesting.

Acknowledgments

The authors are grateful to the Geoscience Laboratories (Sudbury, Canada) for the analytical facilities of the sediments and the team manager of the University of Lausanne (Switzerland) for rock samples analyses. We sincerely acknowledge Dr. Sandric Lesourd and Dr. Clio Bosia for their constructive comments that permitted to improve considerably our manuscript. The Associate Editor's (François Chabaux) advices were warmly appreciated.

Appendix A. Supplementary data

Supplementary data associated with this article can be found, in the online version, at https://doi.org/10.1016/j.crte.2017.08.003.

References

Ahmad, A.H.M., Noufal, K.N., Masroor, A.M., Tavheed, K., 2014. Petrography and geochemistry of Jumara Dome sediments, Kachchh Bas: implications for provenance, tectonic setting and weathering intensity. Chin. J. Geochem 33, 009–023.

Ali, S., Stattegger, K., Garbe-Schöngerg, D., Frank, M., Kraft, S., Kuhnt, W., 2014. The provenance of Cretaceous to Quaternary sediments in the Tarfaya basin, SW Morocco: evidence from trace element geochemistry and radiogenic Nd-Sr isotopes. J. Afr. Earth Sci. 90, 64–76.

Armstrong-Altrin, J.S., Lee, Y.I., Kasper-Zubillaga, J.J., Carranza-Edwards, A., Garcia, D., Eby, G.N., Balaram, V., Cruz-Ortiz, N.L., 2012. Geochemistry of beach sands along the western Gulf of Mexico, Mexico: implication for provenance. Chem. Erde Geochem. 72, 345–362.

Armstrong-Altrin, J.S., Lee, Y.I., Verma, S.P., Ramasamy, S., 2004. Geochemistry of sandstones from the upper Miocene Kudankulam Formation, southern India: implications for provenance, weathering, and tectonic setting. J. Sediment. Res. 74, 285–297.

Armstrong-Altrin, J.S., Machain-Castillo, M.L., Rosales-Hoz, L., Carranza-Edwards, A., Sanchez-Cabeza, J.-A., Ruíz-Fernández, A.C., 2015. Provenance and depositional history of continental slope sediments in the southwestern Gulf of Mexico unraveled by geochemical analysis. Cont. Shelf Res. 95, 15–26.

Asadi, S., Moore, F., Keshavarzi, B., 2013. The nature and provenance of Golestan loess deposits in Northeast Iran. Geol. J. 48, 646–660.

Bassis, A., Hinderer, M., Meinhold, G., 2016. New insights into the provenance of Saudi Arabian Palaeozoic sandstones from heavy mineral analysis and single-grain geochemistry. Sediment. Geol. 333, 100–114.

Bhat, M.I., Ghosh, S.K., 2001. Geochemistry of the 2.51 Ga old Rampur group pelites, western Himalayas: implications for their provenance and weathering. Precambr. Res. 108, 1–16.

Borrego, J., López-González, N., Carro, B., Lozano-Soria, O., 2005. Geochemistry of rare-earth elements in Holocene sediments of an acidic estuary: environmental markers (Tinto River Estuary, South Spain). J. Geochem. Explor. 86, 119–129.

Bouyo, M.H., Zhao, Y., Penaye, J., Zhang, S.H., Njel, U.O., 2015. Neoproterozoic subduction-related metavolcanic and metasedimentary rocks from the Rey Bouba Greenstone Belt of north-central Cameroon in the Central African Fold Belt: new insights into a continental arc geodynamic setting. Precambr. Res. 261, 40–53.

Braun, J.J., Ndam, J.R., Viers, J., Dupré, B., Bedimo Bedimo, J.P., Freydier, R., Sigha Nkamdjou, L., Robain, H., Boeglin, J.L., Muller, J.P., 2005. Present weathering mass balance in lowland tropical humid ecosystem: site of Nsimi (South Cameroon). Geochim. Cosmochim. Acta 69, 7357–7387.

Champetier de Ribes, G., Aubague, M., 1956. Carte géologique de reconnaissance à l'échelle du 1/500 000 + notice explicative sur la feuille Yaoundé-Est. (35 p.).

Cherniak, J.D., Manchester, J., Watson, B.E., 2007. Zr and Hf diffusion in rutile. Earth Planet. Sci. Lett. 261, 267–279.

Cook, S.J., Fletcher, W.K., 1993. Distribution and behaviour of platinum in soils, sediments and waters of the Tulameen ultramafic complex, southern British Columbia, Canada. J. Geochem. Explor. 46 (3), 279–308.

Cullers, R.L., Barrett, T., Carlson, R., Robinson, B., 1987. Rare earth element and mineralogic changes in Holocene soil and stream sediment: a case study in the Wet Mountains, Colorado, USA. Chem. Geol. 63, 275–297.

Duran, C.J., Barnes, S.-J., Corkery, J.T., 2015. Chalcophile and platinum-group element distribution in pyrites from the sulfide-rich pods of the Lac des Iles Pd deposits, western Ontario, Canada: implications for post-cumulus re-equilibration of the ore and the use of pyrite compositions in exploration. J. Geochem. Explor. 158, 223–242.

Etemad-Saeed, N., Hosseini-Barzi, M., Armstrong-Altrin, J.S., 2011. Petrography and geochemistry of clastic sedimentary rocks as evidence for provenance of the Lower Cambrian Lalun Formation, Posht-e-badam block, Central Iran. J. Afr. Earth Sci. 61, 142–159.

Fedo, C.M., Nesbitt, H.W., Young, G.M., 1995. Unraveling the effects of potassium metasomatism in sedimentary rocks and paleosoils, with implications for paleoweathering conditions and provenance. Geology 23, 921–924.

Garver, J.I., Royce, P.R., Smick, T.A., 1996. Chromium and nickel in shale of the Taconic Foreland: a case study for the provenance offine-grained sediments with an ultramafic source. J. Sediment. Res. 66, 100–106.

Kanouo, S.N., Yongue-Fouateu, R., Chen, S., Njonfang, E.M.C., Ghogomu, R.T., Zhao, J., Sababa, E., 2012. Greyish-black megaclasts from the Nsanaragati gem placer, SW Cameroon: geochemical features and genesis. J. Geogr. Geol. 4 (2), 134–146.

Kasanzu, C., Maboko, M.A.H., Manya, S., 2008. Geochemistry of fine-grained clastic sedimentary rocks of the Neoproterozoic Ikorongo Group, NE Tanzania: implications for provenance and source rock weathering. Precambr. Res. 164, 201–213.

Le Goff, E., Deschamp, Y., Guerrot, C., 2010. Tectonic implications of new single zircon Pb–Pb evaporation data in the Lossogonoi and Longido ruby-districts, Mozambican metamorphic Belt of north-eastern Tanzania. C. R. Geoscience 342, 36–45.

Letouzey, R., 1985. Notice explicative de la carte phytogéographique du Cameroun à l'échelle de 1/50 0000. Fascicules 1, 2, 3, 4 et 5. Institut de la carte Internationale de la végétation. Univ. Paul Sabatier, Toulouse (240 p.).

Li, Q., Liu, S., Han, B., Zhang, J., Chu, Z., 2005. Geochemistry of metasedimentary rocks of the Proterozoic Xingxingxia complex: implications for provenance and tectonic setting of the eastern segment of the central Tianshan tectonic zone, northwestern China. J. Afr. Earth Sci. 42, 287–306.

Liu, Z., Zhao, Y., Colin, C., Stattegger, K., Wiesner, M.G., Huh, C.-A., Zhang, Y., Li, X., Sompongchaiyakul, P., You, C.-F., Huang, C.-Y., Liu, J.T., Siringan, F.P., Le, K.P., Sathiamurthy, E., Hantoro, W.S., Liu, J., Tuo, S., Zhao, S., Zhou, S., He, Z.W.Y., Bunsomboonsakul, S., Li, Y., 2016. Source-to-sink transport processes of fluvial sediments in the South China Sea. Earth Sci. Rev. 153, 238–273.

Long, X., Yuan, C., Sun, M., Safonova, I., Xiao, W., Yujing, W., 2012. Geochemistry and U-Pb detrital zircon dating of Paleozoic graywackes in East Junggar, NW China: insights into subduction–accretion processes in the southern Central Asian Orogenic Belt. Gondwana Res. 21, 637–653.

Malkovets, V.G., Rezvukhin, D.I., Belousova, E.A., Griffin, W.L., Sharygin, I.S., Tretiakova, I.G., Gibsher, A.A., O'Reilly, S.Y., Kuzmin, D.V., Litasov, K.D., Logvinova, A.M., Pokhilenko, N.P., Sobolev, N.V., 2016. Cr-rich rutile: a powerful tool for diamond exploration. Lithos 265, 304–311.

Martins, R., Azevedo, M.R., Mamede, R., Sousa, B., Freitas, R., Rocha, F., Quintino, V., Rodrigues, A.M., 2012. Sedimentary and geochemical characterization and provenance of the Portuguese continental shelf soft-bottom sediments. J. Mar. Syst. 91, 41–52.

Maurizot, P., Abessolo, A., Feybesse, A., Johan, V., Lecomte, P., 1986. Étude et prospection minière du Sud-Ouest Cameroun. Synthèse des travaux de 1978 à 1985. 85-CMR 066 BRGM. .

McDonough, W.F., Sun, S.S., 1995. The composition of the Earth. Chem. Geol. 120, 223–253.

McLennan, S.M., 1989. Rare earth elements in sedimentary rocks: influence of provenance and sedimentary processes. In: Lipin, B.R., McKay, G.A. (Eds.), Geochemistry and mineralogy of rare earth elements. Rev. Mineral. 21, 169–200.

McLennan, S.M., 1993. Evolution of the Earth's surface. J. Geol. 101 (2), 295–303.

Meinhold, G., 2010. Rutile and its application in earth sciences. Earth. Sci. Rev. 102, 1–28.

Meinhold, G., Andres, B., Kostopoulos, D., Reischmann, T., 2008. Rutile chemistry and thermometry as provenance indicator: an example from Chios Island, Greece. Sediment. Geol. 203, 98–111.

Merten, D., Geletneky, J., Bergmann, H., Haferburg, G., Kothe, E., Büchel, G., 2005. Rare earth elements patterns: a tool for understanding processes in remediation of acid mine drainage. Chem. Erde Geochem. 65, 97–114.

Meyer, M., John, T., Brandt, S., Klemd, R., 2011. Trace element composition of rutile and the explanation of Zr in rutile thermometry to UHT metamorphism (Epupa Complex, NW Namibia). Lithos 126, 388–401.

Miller, C., Zanetti, A., Thoni, M., Konzett, J., 2007. Eclogitisation of gabbroic rocks: redistribution of trace elements and Zr in rutile thermometry in an Eo-Alpine subduction zone (Eastern Alps). Chem. Geol. 239 (1–2), 96–123.

Morton, A.C., Hallsworth, C.R., 1999. Processes controlling the composition of heavy mineral assemblages in sandstones. Sediment. Geol. 124, 3–30.

Moufti, A.M.B., 2014. Opaque mineralogy and resource potential of placer gold in the stream sediments between Duba and Al Wajh, Red Sea coast, northwestern Saudi Arabia. J. Afr. Earth Sci. 99, 188–201.

Muhammad, A., Mansoor, K., 2015. Study of alluvial gold sediments of river Kabul, district Nowshera (Khyber Pakhtunkhwa, Pakistan). Int. J. Technol. Res. Appl. 23, 77–83.
Nagarajan, R., Madhavaraju, J., Armstrong-Altrin, J.S., Nagendra, R., 2011. Geochemistry of Neoproterozoic limestones of Shahabad Formation, Bhima basin, Karnataka, southern India. Geosci. J. 15, 9–25.
Neal, C.R., Taylor, L.A., 1989. A negative Ce anomaly in a peridotite xenolith: evidence for crustal recycling into the mantle or mantle metasomatism. Geochim. Cosmochim. Acta 53, 1035–1040.
Nesbitt, H.W., Young, G.M., 1982. Early Proterozoic climates and plate motions inferred from major element chemistry of lutites. Nature 299, 715–717.
Nesbitt, H.W., Young, G.M., 1984. Prediction of some weathering trends of plutonic and volcanic rocks based on thermodynamic and kinetic consideration. Geochim. Cosmochim. Acta 48, 1523–1534.
Nzenti, J.P., Barbey, P., Macaudière, J., Soba, D., 1988. Origin and evolution of the Late Precambrian high-grade Yaoundé gneisses (Cameroon). Precambr. Res. 38, 91–109.
Owona, S., Shulz, B., Ratschbacher, L., Mvondo Ondoa, J., Ekodeck, G.E., Tchoua, F.M., Affaton, P., 2011. Pan-African metamorphic evolution in the southern Yaoundé Group (Oubanguide Complex, Cameroon) as revealed by EMP-Monazite dating and thermobarometry of garnet metapelites. J. Afr. Earth Sci. 59, 125–139.
Penaye, J., Toteu, S.F., Van Schmus, W.R., Nzenti, J.P., 1993. U-Pb and Sm-Nd preliminary geochronologic data on the Yaoundé Group, Cameroon: re-interpretation of the granulitic rocks as the suture of a collision in the ''Centrafrican belt''. C. R. Acad. Sci. Paris, Ser. II 317, 789–794.
Prego, R., Caetano, M., Bernardez, P., Brito, P., Ospina-Alvarez, N., Vale, C., 2012. Rare earth elements in coastal sediments of the northern Galician Shelf: influence of geological features. Cont. Shelf Res. 35, 75–85.
Ronov, A.B., Balashov, Y.A., Girin, Y.P., Bratishko, R.K.H., Kazakov, G.A., 1974. Regularities of rare earth element distribution in the sedimentary shell and in the crust of the earth. Sedimentology 21, 171–193.
Roux, P.J., Rojax, M.E., 2007. Sediment transport patterns determined from grain size parameters: overview and state of art jour. Sediment. Geol. 202, 473–488.
Saleh, G.M., 2007. Geology and rare-earth element geochemistry of highly evolved, molybdenite-bearing granitic plutons, southeastern Desert, Egypt. Chin. J. Geochem. 26 (4), 333–344.
Schwertmann, U., 1971. Transformation of haematite to goethite in soils. Nature 232 (5313), 624–625.
Shao, J.Q., Yang, S.Y., 2012. Does chemical index of alteration (CIA) reflect silicate weathering and monsoonal climate in the Changjiang River basin? Chin. Sci. Bull. 57, 1178–1187.
Shao, J., Yang, S., Li, C., 2012. Chemical indices (CIA and WIP) as proxies for integrated chemical weathering in China: inferences from analysis of fluvial sediments. Sediment. Geol. 265–266, 110–120.
Silva, M.M.V.G., Lopes, S.P., Gomesa, E.C., 2014. Geochemistry and behavior of REE in stream sediments close to an old Sn-W mine, Ribeira, Northeast Portugal. Chem. Erde Geochem. 74, 545–555.
Silva, M.V.M.G., Pinto, M.M.S.C., Carvalho, P.C.S., 2016. Major, trace and REE geochemistry of recent sediments from lower Catumbela River (Angola). J. Afr. Earth Sci. 115, 203–217.
Simonet, C., Fritsch, E., Lasnier, B., 2008. A classification of gem corundum deposits aimed towards gem exploration. Ore. Geol. Rev. 34, 127–133.
Šmuc, N.R., Serafimovski, T., Dolenec, T., Dolenec, M., Vrhovnik, P., Vrabec, M., Jačimović, R., Zorn, V.L., Komar, D., 2015. Mineralogical and geochemical study of Lake Dojran sediments (Republic of Macedonia). J. Geochem. Explor. 150, 73–83.
Song, Y.-H., Choi, M.S., 2009. REE geochemistry of fine-grained sediments from major rivers around the Yellow Sea. Chem. Geol. 266, 328–342.
Stendal, H., Toteu, S.F., Frel, R., Penaye, J.U.O., Bassahak, J., Kankeu, B., Ngako, V., Hell, J., 2006. Derivation of rutile in the Yaoundé region from the Neoproterozoic Pan-African belt in southern Cameroon (Central Africa). J. Afr. Earth Sci. 44, 443–458.
Tanis, E.A., Simon, A., Zhang, Y., Chow, P., Xiao, Y., Hanchar, J.M., Tschauner, O., Shen, G., 2016. Rutile solubility in NaF-NaCl-KCl-bearing aqueous fluids at 0.5–2.79 GPa and 250–650 °C. Geochim. Cosmochim. Acta 177, 170–181.
Tonje, J.C., Ndjigui, P.D., Nyeck, B., Bilong, P., 2014. Geochemical features of the Matomb alluvial rutile from the Neoproterozoic Pan-African belt, southern Cameroon. Chem. Erde Geochem. 74, 557–570.
Toteu, S.F., Van Schmus, R.W., Penaye, J., Michard, A., 2001. New U-Pb and Sm-Nd data from north-central Cameroon and its bearing on the pre-Pan-African history of central Africa. Precambr. Res. 108, 45–73.
Traoré, D., Beauvais, A., Augé, T., Chabaux, F., Parisot, J.-C., Cathelineau, M., Peiffert, C., Colin, F., 2006. Platinum and palladium mobility in supergene environment: the residual origin of the Pirogues River mineralization, New Caledonia. J. Geochem. Explor. 88 (1–3), 350–354.
Wang, S., Zhang, N., Chen, H., Li, L., Yan, W., 2014. The surface sediment types and their rare earth element characteristics from the continental shelf of the northern South China sea. Cont. Shelf Res. 88, 185–202.
White, W.M., 2013. Geochemistry. Wiley-Blackwell, 660 p.
Wronkiewicz, D.J., Condie, K.C., 1990. Geochemistry and mineralogy of sediments from the Ventersdorp and Transvaal Supergroups, South Africa: Cratonic evolution during the Early Proterozoic. Geochim. Cosmochim. Acta 54, 343–354.
Zack, T., Kronz, A., Foley, S.F., Rivers, T., 2002. Trace element abundances in rutile from redistribution of trace elements and Zr in rutile thermometry in an Eo-Alpine subduction zone (Eastern Alps). Chem. Geol. 239, 96–123.
Zack, T., Moraes, R., Kronz, A., 2004. Temperature dependence of Zr in rutile: empirical calibration of a rutile thermometer. Contrib. Mineral. Petrol. 148, 471–488.
Zaid, S.M., Gahtani, F.A., 2015. Provenance, diagenesis, tectonic setting and geochemistry of Hawkesbury sandstone (Middle Triassic), southern Sydney Basin, Australia. Turk. J. Earth Sci. 24, 72–98.